Received: 7 May 2015 | Revised: 17 August 2016 | Accepted: 10 October 2016

DOI 10.1002/stc.1961

WILEY

RESEARCH ARTICLE

Online structural damage identification technique using constrained dual extended Kalman filter

Subhamoy Sen | Baidurya Bhattacharya

Civil Engineering Department, Indian Institute of Technology Kharagpur, Kharagpur, West Bengal, India

Correspondence
Baidurya Bhattacharya, Civil Engineering Department, Indian Institute of Technology Kharagpur, Kharagpur, West Bengal, India.
Email: baidurya@civil.iitkgp.ernet.in

Summary

Periodic health assessment of large civil engineering structures is an effective way to ensure safe performance all through their service lives. Dynamic response-based structural health assessment can only be performed under normal/ambient operating conditions. Existing Kalman filter-based parameter identification algorithms that consider parameters as the only states require the measurements to be sufficiently clean in order to achieve precise estimation. On the other hand, appending parameters in an extended state vector in order to jointly estimate states and parameters is reported to have convergence issues. In this article, a constrained version of the dual extended Kalman filtering (cDEKF) technique is employed in which two concurrent extended Kalman filters simultaneously filter the measurement response (as states) and estimate the elements of state transition matrix (as parameters). Constraints are placed on stiffness and damping parameters during the estimation of the gain matrix to ensure they remain within realistic bounds. The proposed method is compared against the existing Kalman filter-based parameter identification techniques on a three-degrees-of-freedom mass-spring-damper system adopting both unconstrained and constrained estimation approaches. cDEKF is then employed on a numerical six-story shear frame and a 3D space truss to validate its robustness and efficacy in identifying structural damage. The results suggest that cDEKF algorithm is an efficient online damage identification scheme that makes use of ambient vibration response.

KEYWORDS

dual extended Kalman filter, constrained Kalman filter, online damage detection, structural health monitorin

1 | INTRODUCTION

Online health monitoring of civil infrastructure systems enables real-time identification of damage and thus helps maintain a system above required levels of safety. In general, any structural health monitoring system comprises of three major components (a) a network of sensors, (b) a response data acquisition system to record the structural response, and (c) a computationally inexpensive health assessment algorithm to detect abnormal changes in the structure.[1,2]

In systems research, control theory-based fault identification under uncertainty has been prevalent over last few decades. The adoption of such control-based techniques in structural health monitoring is challenging, owing to the relatively large system sizes and the necessity of system identification in an uncontrolled noisy environment. Sequential data assimilation-based Bayesian filtering techniques have been successfully employed[3–6] in this attempt. Of the different kinds of Bayesian filters used for state and/or parameter estimation, the Kalman filter (KF)[7] is the most widely used approach owing to the simplicity of the estimation procedure. In KF, the system is defined through a set of states that are observed through a set of measurements. The state estimates are propagated in time using a process model. This prior information is then updated using the new information in the current measurement.

1.1 | Kalman filter for parameter identification

KF has been successfully applied to a wide variety of control problems,[8,9] for example, signal filtering, subject tracking, system control, and so forth. Besides, it has also been extensively applied in parameter identification problems in which a set of model parameters is considered as the system states and observed through model-predicted response. This approach demands a nonlinear mapping of parameters to measurements, which makes the parameter estimation problem nonlinear.

Because KF is a linear state estimator, it cannot be employed for nonlinear system estimation. Nonlinear variants of KF (e.g., extended KF (EKF), unscented KF (UKF), etc.) are capable of dealing with nonlinearity either by local linearization of the system using Taylor series expansion (EKF)[10] or by propagating the first two moments of states through suitably selected sigma points and corresponding weights (UKF).[11,12] Hoshiya et al.[3] applied EKF for structural parameter identification and later several others used similar approaches for different types of parameter identification problems on linear time invariant systems.[4,6,13,14] Yang et al.[15] developed adaptive tracking using EKF to estimate structural damage online, which was later implemented on systems with known[16] and unknown inputs.[17] Other variants of KF for health monitoring purposes, for example, UKF,[18] particle filter,[19] Monte-Carlo filter,[20] and so forth, also exist in the literature.

However, for both linear and nonlinear time-varying systems, in which the system undergoes drastic changes over a small time interval, the application of these filters can be disastrous. This is due to the fact that as the parameters are identified over time in an optimal sense, on introduction of sudden change in the system, the solution may leave the optimal range and can even diverge resulting in completely unrealistic solutions. This necessitates dual and simultaneous estimation of states and parameters for time-varying systems.

1.2 | Dual estimation of state and parameter

Existing applications of dual estimation consider states and parameters jointly in an extended state vector of a joint bilinear state space formulation. Subsequently, EKF is employed to identify the extended state vector. This approach is commonly referred to as the joint EKF (JEKF) technique.[21–23] JEKF, however, has issues with the convergence of the solution.[24] Ljung[25,26] attributes this fault to the simplified gradient calculation of the state transition function with respect to parameter keeping the states constant. Nelson[27] blames the crude linearization of the higher order coupling between states and parameters for this improper convergence. To avoid this coupling issue, Nelson[27] used two separate KFs for states and parameters. However, due to the assumed linearity in the system, this approach loses practicality for nonlinear systems.

Wan[28,29] introduced dual-EKF or DEKF as a nonlinear extension of Nelson's dual KF[27] for simultaneous estimation of states and parameters. Application of DEKF algorithm is, however, limited in literature. Existing applications of DEKF are performed in the fields of vehicular motion control,[30] reservoir monitoring,[31] speech recognition,[29] battery management,[32] and so forth. To our knowledge, no study exists on DEKF for structural damage detection. This article employs DEKF for online structural damage identification using ambient vibration response. Unlike other problems already explored with the DEKF algorithm, the state space representation of civil infrastructure systems is larger and more complex, which necessitates certain constraints to be imposed in the solution procedure in order to obtain a practical solution.

In this article, the proposed constrained DEKF (or cDEKF) method is compared with EKF-based parameter identification algorithms with parameters as either the only states (termed as parameter EKF or PEKF in this article) or a subset of the extended state vector (JEKF), and attempts are made to identify possible complications that may arise in the application of those approaches. The proposed cDEKF algorithm is employed on two numerical examples: (a) a six-story shear frame and (b) a large truss bridge (40 nodes and 152 members). While the first example attempts to demonstrate the method explicitly, the latter explores the proposed method's applicability in large structures. The possibility of raising any false alarm is also investigated in this endeavor.

2 | BACKGROUND

The dynamics of any generalized stochastic system (linear or nonlinear) can be described in its state space domain by a set of process and measurement equation as

$$\begin{aligned} \text{Process equation:} \quad & \dot{\mathbf{x}}(t) = f(\mathbf{x}(t), \theta(t)) + \mathbf{v}^{\mathbf{x}}(t); \\ \text{Measurement equation:} \quad & \mathbf{y}(t) = h(\mathbf{x}(t), \theta(t)) + \mathbf{w}^{\mathbf{x}}(t) \end{aligned} \tag{1}$$

where $\mathbf{x}(t)$ and $\mathbf{y}(t)$ are the state and measurement vectors, respectively. $\theta(t)$ is the time-varying parameter of the system. $\mathbf{v}^x(t)$ and $\mathbf{w}^x(t)$ are process and measurement noise modeled as uncorrelated Gaussian.$f(\bullet)$ and $h(\bullet)$ are the state transition function and measurement function, respectively, which can be replaced by their corresponding Jacobians:

$$\mathbf{A}_c(t) = \frac{\partial f(\mathbf{x}(t), \theta(t))}{\partial x}\Big|_{\mathbf{x}(t)} \text{ and } \mathbf{C}_c(t) = \frac{\partial h(\mathbf{x}(t), \theta(t))}{\partial x}\Big|_{\mathbf{x}(t)}$$

around the current states as their locally linearized surrogate models. Thus, the equivalent linearized system dynamics can be presented as

$$\begin{aligned} \dot{\mathbf{x}}(t) &= \mathbf{A}_c(t)\mathbf{x}(t) + \mathbf{v}^x(t); \\ \mathbf{y}(t) &= \mathbf{C}_c(t)\mathbf{x}(t) + \mathbf{w}^x(t) \end{aligned} \tag{2}$$

For general mechanical systems, the state transition matrix $\mathbf{A}_c(t)$ can be expanded as

$$\mathbf{A}_c(t) = \begin{bmatrix} \mathbf{z}_n & \mathbf{I}_n \\ -\mathbf{M}(t)^{-1}\mathbf{K}(t) & -\mathbf{M}(t)^{-1}\mathbf{D}(t) \end{bmatrix} \tag{3}$$

where $\mathbf{z}_n$ and $\mathbf{I}_n$ are nth order null and identity matrices, respectively, and $\mathbf{M}(t)$, $\mathbf{K}(t)$, $\mathbf{D}(t)$ are the system's mass, stiffness, and damping matrices, respectively.[33]

The continuous time state transition matrix $\mathbf{A}_c(t)$ is relatively more interpretable than its discrete counterpart because detailed information about the structural stiffness can be obtained by exploiting its structure as given in Equation (3). However, as the estimation is performed in discrete time domain using sampled measurement, this formulation should be transformed accordingly. Toggling between discrete time domain formulation and its continuous counterpart can be achieved using zero-order hold technique. The discrete counterpart of the system dynamics sampled with a frequency $1/\Delta t$ can be defined for the kth (i.e., $t = k\Delta t$) time instant as

$$\begin{aligned} \mathbf{x}_k &= \mathbf{A}_k \mathbf{x}_{k-1} + \mathbf{v}_k^x; \\ \mathbf{y}_k &= \mathbf{C}_k \mathbf{x}_k + \mathbf{w}_k^x \end{aligned} \tag{4}$$

where $\mathbf{x}_k$, $\mathbf{y}_k$, $\mathbf{A}_k$, $\mathbf{C}_k$, $\mathbf{v}_k^x$, and $\mathbf{w}_k^x$ are the discrete counterparts of the corresponding continuous entities above. Each element of the discrete time state transition matrix $\mathbf{A}_k$ is considered to be a parameter of the system. In this formulation, the process equation describes the time evolution of the states $\mathbf{x}_k$ while the measurement equation maps the unobserved states onto corresponding measurements.

For a given noisy measurement $\mathbf{y}_{1:k}$ (i.e., measurement array for the timespan 1 to k recorded from the system), KF estimates the system states $\mathbf{x}_{k|k}$ ($\mathbf{x}_{i|j}$ defines the estimate of system state $\mathbf{x}$ at ith time instant based on information up to time instant j) by recursively updating the prior estimate of states (i.e., $\mathbf{x}_{k|k-1}$) using the information in the measurement. Because the noise $\mathbf{v}_k^x$ and $\mathbf{w}_k^x$ are uncorrelated Gaussian, Equation (4) describes a Gauss–Markov process in $\mathbf{x}_k$, and hence $\mathbf{x}_k$ has the Markovian property.

$$\rho(\mathbf{x}_k|\mathbf{x}_{k-1}, \ldots, \mathbf{x}_1, \mathbf{x}_0) = \rho(\mathbf{x}_k|\mathbf{x}_{k-1}) \tag{5}$$

In each step of filtering, the updated (or posterior) probability density function $\rho(\mathbf{x}_k|\mathbf{y}_{1:k})$ of the current state $\mathbf{x}_k$ conditioned upon measurements $\mathbf{y}_{1:k}$ can be described as

$$\rho(\mathbf{x}_k|\mathbf{y}_{1:k}) = \alpha \rho(\mathbf{x}_k|\mathbf{y}_{1:k-1}) \rho(\mathbf{y}_k|\mathbf{x}_k) \tag{6}$$

where the Markov property has been used. The $\rho(\mathbf{x}_k|\mathbf{y}_{1:k-1})$ and $\rho(\mathbf{x}_k|\mathbf{y}_{1:k})$ are the prior and posterior probability densities, respectively, of state $\mathbf{x}_k$. $\rho(\mathbf{y}_k|\mathbf{x}_k)$ is the likelihood of observing a measurement $\mathbf{y}_k$ with an estimate of state as $\mathbf{x}_k$. α is a normalizing coefficient.

KF assumes Gaussian distribution for the initial state and the noise terms. Thus, the maximum-a-posteriori estimate corresponds to the mean of the posterior distribution conditioned on the measurements $\mathbf{y}_{1:k}$:

$$\hat{\mathbf{x}}_{k|k} = \underset{\mathbf{x}_k}{arg\ max} \rho(\mathbf{x}_k|\mathbf{y}_{1:k}) \tag{7}$$

$\hat{\mathbf{x}}_{k|k}$ signifies estimate of the state $\mathbf{x}_k$ for a given measurement information up to time step k. Thus for a given measurement, this algorithm estimates only the states of a system for which the system model is explicitly known, which in turn necessitates complete knowledge of the system's parameters. The time evolution of parameters cannot be estimated through this formulation.

2.1 | KF-based parameter estimation

To identify system parameters using KF, the parameters are defined as either the only system states (PEKF) or additional (JEKF) states. In the former approach, the system dynamics is defined using a set of time-invariant parameters θ_k as the system states:

$$\begin{aligned} \theta_k &= \theta_{k-1} + \mathbf{v}_k^\theta; \\ \epsilon_k &= \{\mathbf{y}_k - h(\theta_k)\} + \mathbf{w}_k^\theta \end{aligned} \tag{8}$$

As most parameters of interest are not directly measurable, this approach uses a system model $h(\bullet)$ that maps estimated parameters to measurement to make them observable. In this approach, $\{\mathbf{y}_k - h(\theta_k)\}$ is considered as the measurement function that measures the mismatch ϵ_k between actual measurement $\mathbf{y}_k$ and the model-predicted response $h(\theta_k)$. Because this ignores the filtering of response states $\mathbf{x}_k$, a sufficiently clean measurement becomes a necessity,[23] which is often unavailable.

With parameters appended in the state vector (JEKF), the process equation of the system becomes jointly bilinear as

$$\begin{Bmatrix} \mathbf{x}_k \\ \theta_k \end{Bmatrix} = f\left(\begin{Bmatrix} \mathbf{x}_{k-1} \\ \theta_{k-1} \end{Bmatrix} \right) + \begin{Bmatrix} \mathbf{v}^x \\ \mathbf{v}^\theta \end{Bmatrix}_k \tag{9}$$

where θ_k is the parameter of the system and $\{\mathbf{v}^x \mathbf{v}^\theta\}_k^T$ is Gaussian process noise. The states and parameters can be simultaneously estimated from this formulation as

$$\{\hat{\mathbf{x}}_{k|k}, \hat{\theta}_{k|k}\} = \underset{\{\mathbf{x}_k, \theta_k\}}{arg\ max} \rho(\{\mathbf{x}_k, \theta_k\}|\mathbf{y}_{1:k}) \tag{10}$$

JEKF is demonstrated in Algorithm 1, where the process function f is a simulator model (e.g., finite element (FE) model) to propagate the state estimates to the next time instant and $\mathbf{A}_k$ is the corresponding linearized model at time instant k. Thus in each step of JEKF, a rigorous gradient calculation involves costly FEM simulation, which increases the computational burden.

It has been previously discussed in this article that with augmented (or extended) state vector approach (JEKF), the estimation may suffer from improper convergence (as described by Ljung[25,26] and Nelson[27]). On the other hand, with the decoupled approach (PEKF), the measurement signal is required to be sufficiently clean. Parameter estimation using noisy measurement signals therefore demands a new method so that filtering the noise can be done together with parameter identification. This leads to the proposed constrained DEKF (cDEKF) algorithm as an alternative to the existing dual estimation methods.

Algorithm 1: Joint Extended Kalman Filtering (JEKF) algorithm

Prediction step:
State prediction:
$\{\tilde{\mathbf{x}}_{k|k-1};\tilde{\theta}_{k|k-1}\}^T = f\left(\hat{\mathbf{x}}_{k-1|k-1},\hat{\theta}_{k-1|k-1}\right) = \mathbf{A}_k(\theta)\hat{x}_{k-1|k-1}$
State covariance prediction:
$\tilde{\mathbf{P}}_{k|k-1} = \mathbf{A}_k(\theta)\hat{\mathbf{P}}_{k-1|k-1}\mathbf{A}_k(\theta)^T + \mathbf{Q}_k$;
where $\mathbf{A}_k(\theta) = \nabla_x(f)|_{\hat{\mathbf{x}}_{k-1|k-1},\hat{\theta}_{k-1|k-1}}$

Update step
Measured residual or innovation:
$\epsilon_k = \mathbf{y}_k - h\left(\tilde{\mathbf{x}}_{k|k-1},\tilde{\theta}_{k|k-1}\right)$
Innovation covariance: $\mathbf{S}_k = \mathbf{H}_k\tilde{\mathbf{P}}_{k|k-1}\mathbf{H}_k^T + \mathbf{R}_k$;
where $\mathbf{H}_k = \nabla_x(h)|_{\tilde{\mathbf{x}}_{k|k-1},\tilde{\theta}_{k|k-1}}$

Kalman gain: $\mathbf{K}_k = \tilde{\mathbf{P}}_{k|k-1}\mathbf{H}_k^T\mathbf{S}_k^{-1}$
Update state estimate:
$\{\hat{\mathbf{x}}_{k|k},\hat{\theta}_{k|k}\}^T = \{\tilde{\mathbf{x}}_{k|k-1},\tilde{\theta}_{k|k-1}\}^T + \mathbf{K}_k\epsilon_k$;
update state covariance: $\hat{\mathbf{P}}_{k|k} = (\mathbf{I}-\mathbf{K}_k\mathbf{H}_k)\tilde{\mathbf{P}}_{k|k-1}$

3 | DUAL EXTENDED KALMAN FILTER

The DEKF algorithm applied in this article is due to Wan who introduced this algorithm for the speech recognition problem. This approach has been successfully implemented for dual estimation of the states and parameters in several articles.[29–32] The DEKF algorithm additionally augments Equation 1 with a process model to describe the time evolution of the parameters as

$$\begin{aligned} \mathbf{x}_k &= f(\mathbf{x}_{k-1},\theta_{k-1}) + \mathbf{v}_k^{\mathbf{x}};\\ \theta_k &= \theta_{k-1} + \mathbf{v}_k^{\theta};\\ \epsilon_k &= \{\mathbf{y}_k - h(\mathbf{x}_k,\theta_k)\} + \mathbf{w}_k^{\mathbf{x}} \end{aligned} \tag{11}$$

where θ_k is an array of elements $\mathbf{A}_k^{ij}$ (i and j signifies row and column number) of state transition matrix $\mathbf{A}_k$, which is a locally linearized surrogate model of state transition function $f(\mathbf{x}_{k-1},\theta_{k-1})$. $\mathbf{v}_k^{\theta}$ is the process noise related to the additional process model for the parameters. Noise terms $\mathbf{v}_k^{x}$, $\mathbf{v}_k^{\theta}$, and $\mathbf{w}_k^{x}$ are modeled as zero mean Gaussian sequence with covariance matrices $\mathbf{Q}_\theta$, $\mathbf{Q}_x$, and $\mathbf{R}_x$, respectively.

To employ Bayesian estimation to estimate the system states conditioned on current estimates of parameters, the DEKF algorithm expands Equation 10 as

$$\{\hat{\mathbf{x}}_{k|k},\hat{\theta}_{k|k}\} = \underset{\{\mathbf{x}_k,\theta_k\}}{arg\ max}\ \rho(\mathbf{x}_k|\theta_k,\mathbf{y}_{1:k})\rho(\theta_k|\mathbf{y}_{1:k}) \tag{12}$$

which in DEKF is implemented as two separate estimation schemes for the states and the parameters:

$$\begin{aligned} \hat{\mathbf{x}}_{k|k} &= \underset{\mathbf{x}_k}{arg\ max}\ \rho(\mathbf{x}_k|\theta_k,\mathbf{y}_{1:k})\\ \hat{\theta}_{k|k} &= \underset{\theta_k}{arg\ max}\ \rho(\theta_k|\mathbf{y}_{1:k}) \end{aligned} \tag{13}$$

In each step, the algorithm thus toggles between estimating states based on current estimates of parameters and estimating parameters based on current estimates of states.

3.1 | Constrained DEKF algorithm

Although DEKF has been established as an efficient dual estimator for several other fields, the performance of this powerful tool for structural damage detection is not yet much explored. Unlike existing applications of DEKF, the civil infrastructures systems are dimensionally higher and more complex. Detailed models of such systems with high numbers of degrees of freedom (DOFs) are required to monitor their current health. To avoid this curse of dimensionality, an estimation of a reduced-order system has been proposed in Sen and Bhattacharya,[34] which involves a recursive simulation of the system FE model, making it computationally expensive. The alternate option of using the elements of state transition matrix as parameters with the DEKF algorithm without applying any constraints may lead to infeasible solutions with the possibility of triggering false alarm about the structural health. Certain realistic constraints on the probable solution region are therefore required to be incorporated in the algorithm.

Several constrained KF algorithms exist in literature, dealing with hard or soft, equality or inequality, linear or nonlinear constraints.[35–38] Simon[39] presented an extensive review on the existing techniques to constrain KF. To handle equality constraints (such as noise-free measurement, perfect measurement, and perfectly known properties of system), Ungrala *et al.*[40] performed an additional measurement update step to impart the complete measurement information into the estimate. Simon et al.,[41] on the other hand, described a projection technique to employ an equality constraint. Inequality constraints (such as solution boundaries, region of optimal solutions) are also handled in literature deterministically or statistically by different researchers.[42,43]

In KF algorithms, the gain matrix is analytically derived with the objective to minimize the trace of state covariance matrix. The analytical derivation of gain matrix is presented in the appendix (see Appendix). However, because in the proposed approach the constraints are additionally incorporated in the solution during gain estimation, the closed-form solution is no longer available and can only be estimated through optimization. The gain estimation scheme, posed in this approach as a constrained optimization problem, can be described as

$$\underset{\mathbf{K}}{\arg\min}\{\text{trace}\{\mathbf{P} = (\mathbf{I}-\mathbf{KC})\bar{\mathbf{P}}(\mathbf{I}-\mathbf{KC})^T - \mathbf{K}\mathbf{R}_k\mathbf{K}^T\}\}$$

$$\text{Subjected to:}\quad \left\{\begin{array}{l}\text{Inequality constraint: } \underline{\mathbf{x}} \leqslant \hat{\mathbf{x}}_{k|k} \leqslant \bar{\mathbf{x}}\\ \text{and equality constraint: } \mathbf{C}_g\hat{\mathbf{x}}_{k|k} = \mathbf{d}\end{array}\right\} \tag{14}$$

Algorithm 2: Proposed constrained dual extended Kalman filtering algorithm

Step 1: Initial estimates
Initial state estimate: $\hat{\mathbf{x}}_{0|0} = E(\mathbf{x}_0)$ with covariance
$\mathbf{P}_{\mathbf{x}_{0|0}} = E[(\mathbf{x}_0 - \hat{\mathbf{x}}_{0|0})(\mathbf{x}_0 - \hat{\mathbf{x}}_{0|0})^T]$
Initial parameter estimate: $\hat{\theta}_{0|0} = E(\theta_0)$ with covariance
$\mathbf{P}_{\theta_0} = E[(\theta_0 - \hat{\theta}_{0|0})(\theta_0 - \hat{\theta}_{0|0})^T]$

Step 2: Time update of parameters
Parameter prediction: $\tilde{\theta}_{k|k-1}=\hat{\theta}_{k-1|k-1}$
Parameter covariance prediction: $\tilde{\mathbf{P}}_{\theta_{k|k-1}} = \hat{\mathbf{P}}_{\theta_{k-1|k-1}} + \mathbf{Q}_\theta$

Step 3: Time update of state
State prediction: $\tilde{\mathbf{x}}_{k|k-1} = f(\hat{\mathbf{x}}_{k-1|k-1}, \tilde{\theta}_k)$
State covariance prediction: $\tilde{\mathbf{P}}_{\mathbf{x}_{k|k-1}} = \mathbf{A}_k \hat{\mathbf{P}}_{\mathbf{x}_{k-1|k-1}} \mathbf{A}_k^T + \mathbf{Q}_x$

Step 4: Measurement update of state
Kalman gain matrix for states:
$\mathbf{K}_k^x = \tilde{\mathbf{P}}_{\mathbf{x}_{k|k-1}} \mathbf{C}^T(\mathbf{C}\tilde{\mathbf{P}}_{\mathbf{x}_{k|k-1}}\mathbf{C}^T + \mathbf{R}_x)^{-1}$
State estimate update: $\hat{\mathbf{x}}_{k|k} = \tilde{\mathbf{x}}_{k|k-1} + \mathbf{K}_k^x(\mathbf{y}_k - \mathbf{C}\tilde{\mathbf{x}}_{k|k-1})$
State covariance update: $\hat{\mathbf{P}}_{\mathbf{x}_{k|k}} = (\mathbf{I} - \mathbf{K}_k^x\mathbf{C})\tilde{\mathbf{P}}_{\mathbf{x}_{k|k-1}}$
if {State estimate is within solution boundaries}:
Proceed to Step 5.
else if {predicted estimate is outside solution boundaries}:
$\arg\min_{\mathbf{K}_k^x}\{\text{trace}\{(\mathbf{I} - \mathbf{K}_k^x\mathbf{C})\tilde{\mathbf{P}}_{\mathbf{x}_{k|k-1}}(\mathbf{I} - \mathbf{K}_k^x\mathbf{C})^T - \mathbf{K}_k^x\mathbf{R}_x\mathbf{K}_k^{xT}\}\}$
Subjected to: $\underline{\mathbf{x}} \leq \hat{\mathbf{x}}_{k|k} \leq \overline{\mathbf{x}}$
end

Step 5: Measurement update of parameter
Kalman gain for parameter:
$\mathbf{K}_k^\theta = \tilde{\mathbf{P}}_{\theta_{k|k-1}}\mathbf{C}_k^\theta(\mathbf{C}_k^\theta\tilde{\mathbf{P}}_{\theta_{k|k-1}}\mathbf{C}_k^{\theta T} + \mathbf{R}_\theta)^{-1}$
Parameter estimate update: $\hat{\theta}_{k|k} = \tilde{\theta}_{k|k-1} + \mathbf{K}_k^\theta(\mathbf{y}_k - \mathbf{C}\tilde{\mathbf{x}}_{k|k-1})$
Parameter covariance update: $\hat{\mathbf{P}}_{\theta_{k|k}} = (\mathbf{I} - \mathbf{K}_k^\theta\mathbf{C})\tilde{\mathbf{P}}_{\theta_{k|k-1}}$
if {Parameter estimate is within solution boundaries}:
Proceed to Step 2.
else if {predicted estimate is outside solution boundaries}:
$\arg\min_{\mathbf{K}_k^\theta}\{\text{trace}\{(\mathbf{I} - \mathbf{K}_k^\theta\mathbf{C}_k^\theta)\tilde{\mathbf{P}}_{\theta_{k|k-1}}(\mathbf{I} - \mathbf{K}_k^\theta\mathbf{C}_k^\theta)^T - \mathbf{K}_k^\theta\mathbf{R}_{\theta\mathbf{K}_k^\theta}^T\}\}$
Subjected to: $\underline{\theta} \leq \hat{\theta}_{k|k} \leq \overline{\theta}$
end

$\mathbf{A}_{k-1} = \frac{\partial f(\hat{\mathbf{x}}_{k-1|k-1}, \hat{\theta}_{k-1|k-1})}{\partial x}$;
$\mathbf{C}_k^\theta = -\frac{\partial(\mathbf{y}_k - \mathbf{C}\tilde{\mathbf{x}}_{k|k-1})}{\partial\theta}|_{\theta=\hat{\theta}_{k|k}} = \mathbf{C}\frac{\partial\tilde{\mathbf{x}}_{k|k-1}}{\partial\theta}|_{\theta=\hat{\theta}_{k|k}}$.
$\mathbf{Q}_\theta$, $\mathbf{Q}_x$, $\mathbf{R}_\theta$, $\mathbf{R}_x$ are the process and measurement error covariance matrices for parameters and states respectively.

where $\underline{\mathbf{x}}$ and $\overline{\mathbf{x}}$ are the lower and upper prescribed boundaries for the states defined by the user. $\mathbf{C}_g$ is the output matrix for perfect measurement $\mathbf{d}$. Accordingly, in expense of enhanced computation due to optimization, the achieved estimates ensure that the solution never leaves the region of optimality. To handle this augmented computational demand, the optimization-based gain estimation is, however, attempted only when the solution leaves the region of optimality. For the remaining cases, the analytical approach for gain estimation (as described in Appendix) is applied.

Simultaneous estimation of states ($\mathbf{x}_k$) and parameters (θ_k) from the measured response ($\mathbf{y}_k$) constrained within a specified boundary by cDEKF is described in detail in Algorithm 2.

4 | NUMERICAL VALIDATION

Numerical experiments are performed to demonstrate the efficiency of the proposed cDEKF algorithm for structural damage detection. In this attempt, cDEKF employed certain equality and inequality constraints to constrain the estimates within realistic bounds. A set of noise-free signals, considered as perfect measurement, are used as equality constraints. It should be mentioned here that although noise-free signals are mostly unavailable in reality, we have incorporated this to validate the proposed method's efficiency to handle clean measurements, if available (e.g., modal frequency). To employ inequality constraints for the parameters (i.e., the elements of state transition matrix), two discrete time state space models of the system are prepared using the upper and lower bounds of the physical structural parameters. Elements of the state transition matrices of these two models are then used to define the solution bounds for parameter estimates as inequality constraints. Matlab function "*fmincon*" is employed to solve this constrained optimization problem.

Prior to validating the proposed cDEKF algorithm for structural damage assessment problems, it is compared with existing EKF-based (PEKF and JEKF) parameter estimation algorithms that consider physical structural parameters as system states. In this context, the general DEKF algorithm is first compared with PEKF and JEKF to demonstrate the requirement of the constraining strategies in the estimation. The constrained version of DEKF (i.e., the proposed cDEKF) is then compared with the general DEKF (and also with two other JEKF-based constrained estimation techniques) to demonstrate the benefits of this modification. In the following, the proposed cDEKF algorithm is employed to detect damage in two structures: (a) a six-storey building and (b) a bridge truss. Details of these numerical experiments are presented in the following.

4.1 | Numerical experiment 1: comparison of proposed cDEKF with existing algorithms

A three-DOF mass-spring-damper system is considered (see Figure1) to compare the performance of the DEKF-based algorithm with those of PEKF and JEKF. The mass, stiffness, and damping of this three-DOF system are considered to be $125 kg$, $480 kN/m$, and $10 N-sec/m$, respectively. The

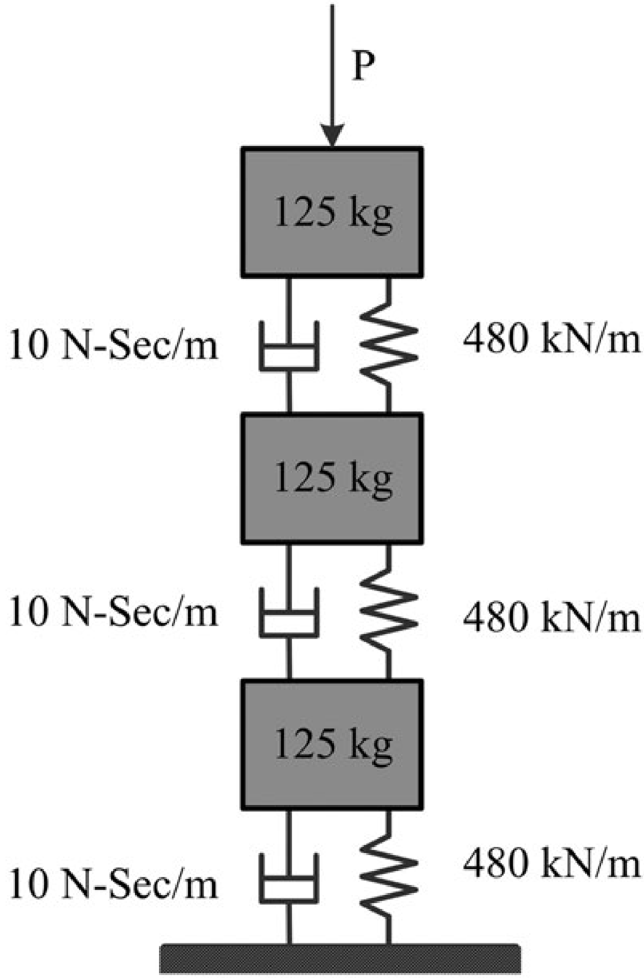

FIGURE 1 Schematic diagram of a three-degree-of-freedom system

system's responses at all free DOFs under external excitation at the third DOF are recorded for a 10-s span with a sampling frequency 1000 Hz and subsequently contaminated with 10% noise. Unconstrained PEKF, JEKF, and DEKF algorithms are then employed to identify two control parameters, that is, stiffness and damping, from this noisy response signal. The size of identifiable state vector for the JEKF algorithm is thus 8 (6 response states and 2 parameter states) and 2 (2 parameter states) for the PEKF case. For the DEKF algorithm, on the other hand, all the 36 elements of state matrix (6×6) are considered as parameter states. Thus, DEKF deals with 36 parameter states and six response states.

Form Figure 2, it can be observed that with noisy signal, the PEKF algorithm performs poorly because it contradicts to its requirement of a sufficiently clean signal. While both JEKF and DEKF estimated the parameters perfectly, DEKF achieved convergence faster than JEKF. However, en route to convergence, the DEKF algorithm estimated some completely unrealistic values (e.g., negative damping value (Figure 2b) and an unusually high value of stiffness (> 5000 kN/m) (Figure 2a)).

To restrict the solution within a practical solution domain, the estimation is further performed with the cDEKF algorithm and compared with existing constrained JEKF algorithms. The assumed solution boundaries are presented here:

$$\begin{gathered} 200kN/m < \text{ Story stiffness} < 600kN/m \\ 1 \times 10^{-15} N - Sec./m < \text{ Damping} < 30 N - Sec./m \end{gathered} \tag{15}$$

Two different constraining strategies to incorporate inequality constraints are applied on the JEKF algorithms. The former (JEKF (Clipped)) employs a clipping technique described in Prakash *et al.*[43] In this method, from a set of realizations of state vectors generated using estimated mean and covariance, the samples that fail to satisfy the constraints are clipped. Subsequently, the moments of states are re-estimated from the refined data set and are used as predicted estimates. The second adopted strategy (JEKF (Curtailed)) is due to Simon *et al.*,[44] in which each estimated state pdf is curtailed beyond its prescribed limits in case it leaves the region of optimality. Finally, the proposed cDEKF algorithm is employed and compared against the other two constrained estimation techniques.

Evidently, Figure 3 demonstrates that the proposed method as well as the other two constrained techniques estimated the parameters precisely with intermediate estimations never exceeding the optimal solution boundaries. However, there are additional benefits of cDEKF over the other constrained JEKF algorithms, which are discussed next.

Although the performance of JEKF is satisfactory for this particular problem, during the gradient calculation of state transition function with respect to parameters, the states are kept constant and thus by recursive derivations of states with respect to parameters are avoided. This simplification may have a detrimental effect on the convergence for

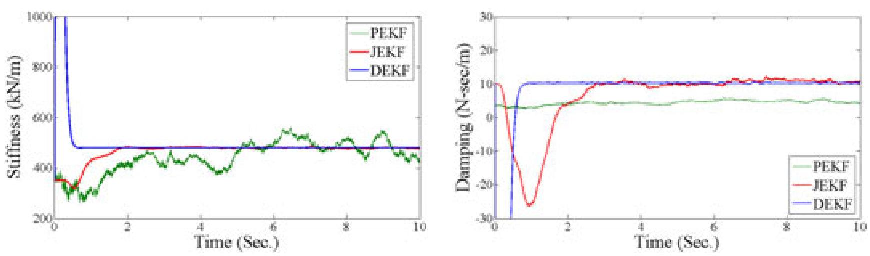

(a) Stiffness estimation (b) Damping estimation

FIGURE 2 Comparison of unconstrained parameter extended Kalman filter (PEKF), joint extended Kalman filter (JEKF), and constrained dual extended Kalman filtering (cDEKF) algorithms

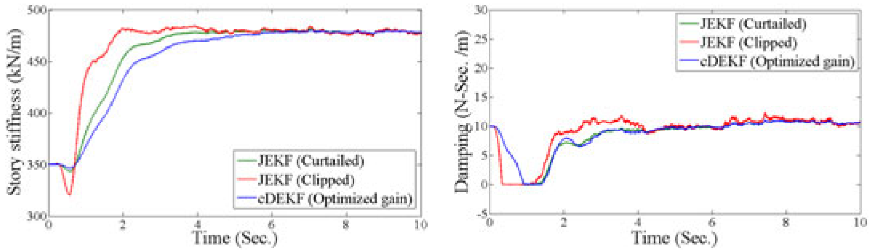

(a) Stiffness estimation (b) Damping estimation

FIGURE 3 Comparison of constrained joint extended Kalman filter (JEKF) (curtailed), JEKF (clipped), and dual extended Kalman filter (DEKF) (optimized gain) algorithms

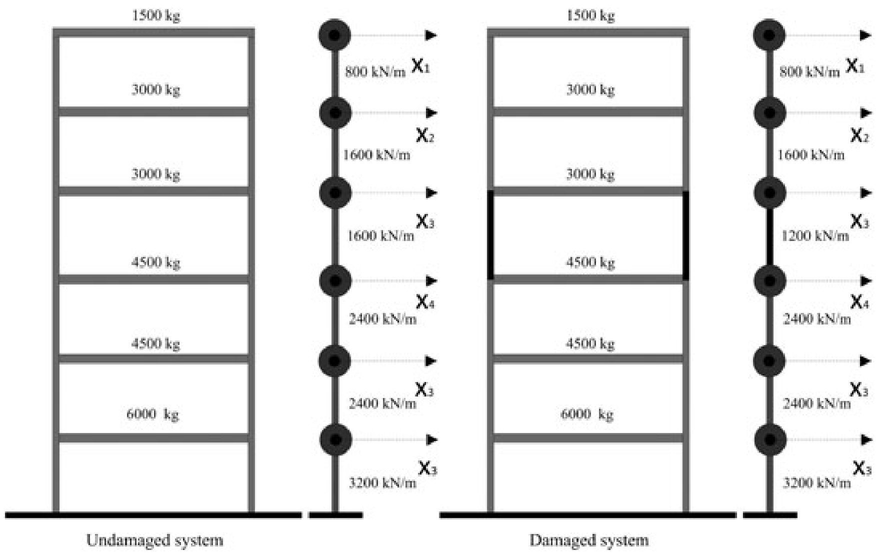

FIGURE 4 Schematic diagram of the damaged and undamaged model of a six-story shear frame

systems with strong coupling between states and parameters. The problem taken up to demonstrate the proposed method's fitness is simple and thus cannot exhibit the convergence issues suffered by the JEKF algorithms. For that, the reader is requested to refer to Nelson and Stear,[27] which incorporates the citations and details related to difficulties in the JEKF approach.

It should also be noted that with the cDEKF algorithm the problem size (36 parameter states and six response states) is larger than the JEKF algorithm (six response states and two parameter states), and it may appear that the cDEKF is complicating the estimation procedure. However, the additional FE modeling step within the JEKF algorithm to propagate the state estimation must be considered because this may cause significant computational burden. On the contrary, cDEKF algorithm does not require any FE modeling step. Thus, even though cDEKF handles problems that are dimensionally larger, its computational demand is always less than that of JEKF algorithms.

4.2 | Numerical experiment 2: six-story shear frame

The second numerical example demonstrates the capability of the cDEKF algorithm to locate structural damage. The system considered for this example is a simple six-story shear frame approximated using a six-DOF lumped mass model (see Figure 4) so that initial and updated matrices can be explicitly presented. The undamaged model is described by stiffness matrix $\mathbf{K}_0$ and mass matrix $\mathbf{M}_0$ with 1% Rayleigh damping.

$$\mathbf{K}_0 = \begin{bmatrix} 800 & -800 & 0 & 0 & 0 & 0 \\ -800 & 2400 & -1600 & 0 & 0 & 0 \\ 0 & -1600 & 3200 & -1600 & 0 & 0 \\ 0 & 0 & -1600 & 4000 & -2400 & 0 \\ 0 & 0 & 0 & -2400 & 4800 & -2400 \\ 0 & 0 & 0 & 0 & 0-2400 & 5600 \end{bmatrix} kN/m; \tag{16}$$

$$\mathbf{M}_0 = diag\{\ 1500\ \ 3000\ \ 3000\ \ 4500\ \ 4500\ \ 6000\ \}kg \tag{17}$$

where "*diag*" is diagonalization operator that creates a sparse matrix with the elements at the diagonal positions.

Assumed modeling details for the undamaged and damaged models are given in Figure 4. Damage is induced in the model by reducing 25% story stiffness of the fourth story. Ambient vibration response is simulated from the damaged model using the Newmark-beta algorithm by exciting all of its six free nodes by a Gaussian white noise, and acceleration

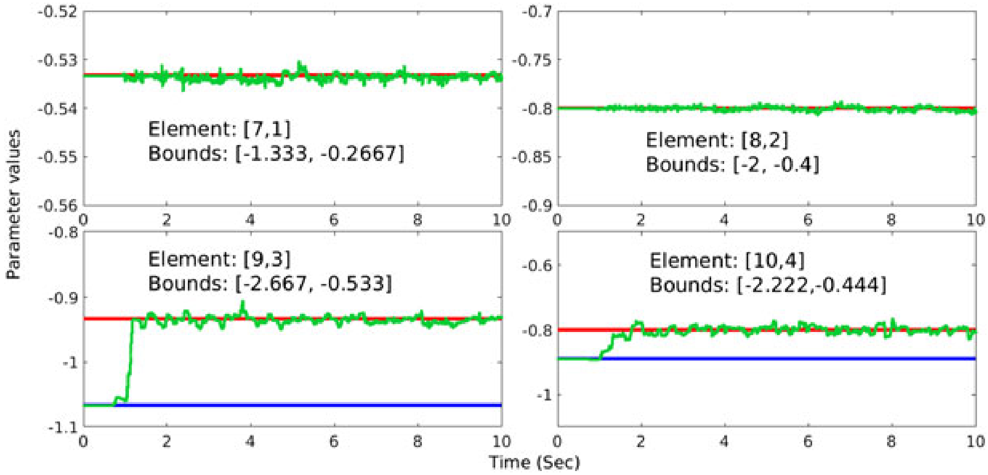

FIGURE 5 Online damage estimation using constrained dual extended Kalman filtering algorithm. Blue and red lines represent the parameter values corresponding to the undamaged and damaged state, respectively. The green line represents the parameter estimation over time. Element numbers, presented in the bracket, are the row-column index of the parameter in the discrete time state transition matrix. The acceptable solution bounds are demonstrated using their higher and lower limits

responses are recorded at a sampling frequency of $1000Hz$ for a time span of 10 s.

Inequality constraints for the state filter are assigned by fixing an estimation boundary two times larger than the noisy signal band. All the 144 elements of the state transition matrix are considered as parameters. However, considering the individual symmetric property in the bottom left and right blocks of state transition matrix, the required number of identified parameters drops down to 114.

For the inequality constraints on parameters, the upper and lower limits (i.e., $\bar{\theta}, \underline{\theta}$) are specified using the following boundaries in story stiffness.

$$\begin{aligned} \underline{\mathbf{k}} &= \{\ 500\ 500\ 500\ 500\ 500\ 500\ \} kN/m \\ \text{and } \bar{\mathbf{k}} &= \{\ 2000\ 2000\ 2000\ 2000\ 2000\ 2000\ \} kN/m \end{aligned} \tag{18}$$

For the equality constraints on states, one out of six measured signals is considered to be perfectly noise free. The cDEKF algorithm is subsequently applied on the noisy measurement to estimate the parameters in order to assess the current structural health.

Figure 5 demonstrates a sample parameter estimation over time for four diagonal elements of the lower left block of the state transition matrix ([7,1],[8,2],[9,3], and [10,4]). The selection of these four elements is due to their critical positions in the state transition matrix through which the health of the first four DOFs can be interpreted. To avoid confusion, we should mention here that the difference between the elements of discrete time state transiton matrices associated to damage and undamage states are termed in this article as "nodal damage" (cf. Figure 5), which does not mean damage in the nodes of the structure. It rather signifies the deterioration in stiffness in the numerical nodes of its FE model. This idea has been maintained throughout this article.

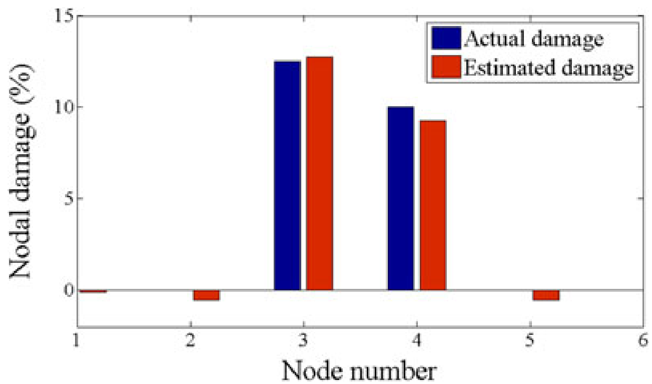

FIGURE 6 Actual and identified nodal damage in the shear frame

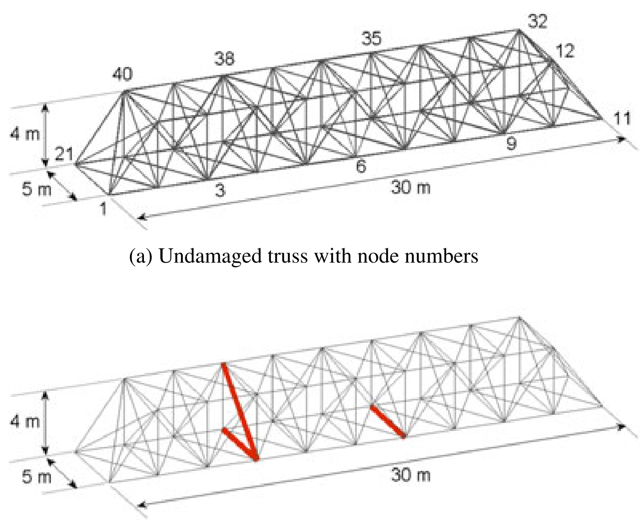

FIGURE 7 Schematic presentation of undamaged and damaged state of the truss

It can be observed that the estimated parameter values never overshot the specified solution boundaries. Eventually, the identified state transition matrix is transferred from discrete time to continuous time domain using the zero-order hold technique. Considering no change in mass matrix due to the induced damage, the updated stiffness matrix ($\mathbf{K}_{id}$) is extracted from which the damage is interpreted by direct comparison against the undamaged stiffness matrix $\mathbf{K}_0$. $\mathbf{K}_{id}$ is given below:

$$\mathbf{K}_{id} = \begin{bmatrix} 797.2 & -803.1 & 0.15 & 0.2 & 0.1 & 0.5 \\ -803.1 & 2400 & -1616.1 & 0.2 & 0.16 & 0.17 \\ 0.15 & -1616.1 & 2794.5 & -1204.2 & 0.24 & 0.32 \\ 0.2 & 0.2 & -1204.2 & 3636.6 & -2413.9 & 0.9 \\ 0.1 & 0.16 & 0.24 & -2413.9 & 4789.6 & -2397.8 \\ 0.5 & 0.17 & 0.32 & 0.9 & -2397.8 & 5591.9 \end{bmatrix} kN/m; \tag{19}$$

The identified damage in each of the nodes of the shear frame is plotted in Figure 6 where it can be seen that the cDEKF algorithm successfully identified the occurrence, location, and intensity of the damage.

4.3 | Numerical experiment 3: space truss

The next numerical example is performed on a 152-member space truss comprising of 120 DOFs (see Figure 7). Details are listed in Table1. Damage in the truss is induced by reducing the undamaged cross section of specific truss members (see Figure 7b). Nine bottom nodes (node numbers 2-10) are instrumented with an accelerometer capable of picking vertical accelerations only. The truss is excited at all 18 top nodes (node numbers 12-20 and 32-40) by a zero-mean Gaussian white noise excitation, and acceleration responses for a time span of 10 s at the instrumented DOFs are simulated using the Newmark-beta algorithm at a sampling frequency of 1000 Hz.

The inequality constraints for parameters are defined by restricting member elasticities between zero (i.e., complete damage) and twice its undamaged value, that is, $4 \times 10^{11} N/m^2$. No equality constraints are used for this numerical example because it is observed that with a high-dimensional problem, too many constraints

TABLE 1 Geometric detailing of the space truss

Member groups	Connectivity	Length (m)	C/S area (cm^2)
1: Stringers	1-2, 2-3, 3-4, 4-5, 5-6, 21-22, 22-23, 23-24, 24-25, 25-26	3	180
2: Top chords	12-13, 13-14, 14-15, 15-16, 32-33, 33-34, 34-35, 35-36	3	463
3: Vertical posts	2-20, 3-19, 4-18, 5-17, 22-40, 23-39, 24-38, 25-37	4	143
4: Diagonal bracing	1-20, 3-20, 3-18, 5-18, 5-16, 21-40, 23-40, 23-38, 25-38, 25-36	5	181
5: Floor beams and struts	20-40, 19-39, 18-38, 17-37, 16-36, 1-21, 2-22, 3-23, 4-24, 5-25	4	463
6: Lateral (wind) bracings	1-22, 2-21, 2-23, 3-22, 3-24, 20-39, 19-40, 19-38, 18-39, 18-37	5	181
7: Sway bracings	1-40, 2-40, 3,39, 4-38, 5-37, 21-20, 20-22, 19-23, 18-24, 17-25	5	181

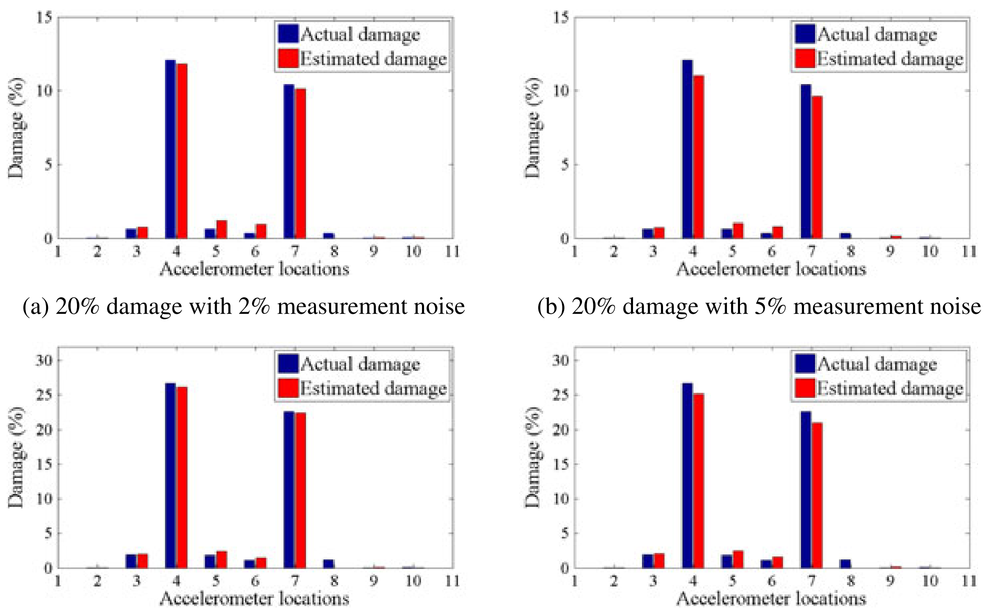

(a) 20% damage with 2% measurement noise

(b) 20% damage with 5% measurement noise

(c) 40% damage with 2% measurement noise

(d) 40% damage with 5% measurement noise

FIGURE 8 Actual and identified damage in the truss for damage in members 4-24, 4-38, and 7-27 in the estimation procedure unnecessarily burden the computation.

Figure 8 presents results of an example problem on the truss with damage in multiple locations. In this example, members 4-24, 4-38, and 7-27 are considered to be damaged. This example is performed for four different conditions involving two different damage severities (20% and 40%) and two different levels of measurement noise (2% and 5% signal to noise). Figure 8 clearly demonstrates that the cDEKF algorithm successfully identified the location of the damage precisely within the sensor resolution. In these figures, the truss is segmented into 10 sections of equal length with nine equally spaced nodes at the accelerometer locations. Subsequently, as per Equation (20), the damage is estimated through the difference in the elements of identified discrete time state transition matrix.

$$\mathbf{d}^{ij} = \frac{A_u^{ij} - A_{id}^{ij}}{A_d^{ij}} \tag{20}$$

where A_u and A_{id} are undamaged and identified state transition matrices, and $\{i,j\}$ signifies the row and column of the corresponding matrix. To identify the location of the damaged node, diagonal elements of the damage matrix $\mathbf{d}$ are plotted in Figure 8. For better comparison, the actual nodal damage derived analytically is also presented in these figures. Figure 8 identifies that the damage has affected the 4th and 7th node the most, which perfectly localizes the damage in the vicinity of the 3rd and 6th accelerometer locations.

4.3.1 | False alarm sensitivity

The susceptibility of the proposed algorithm to false identification is investigated next.[45,46] The space truss structure is subjected to 160 different damage scenarios (eight damage locations × four noise levels × five damage levels), and for each scenario, 100 identifications are performed corresponding to 100 realizations of measurement noise.

We define the "False alarm (FA) index" as the fraction of instances the algorithm resulted in a false prediction of damage in undamaged locations:

$$FA = \frac{1}{N}\sum_{i=1}^{N}\left[1 - \mathbb{I}\{l_{id} = l_{act}\}\right]; \tag{21}$$

l_{act} and l_{id} are the actual and identified damage locations. $\mathbb{I}$ is the indicator function that takes the value 1 if the detected damaged node is truly damaged or zero otherwise.

Results corresponding to 32 of the assumed damage scenarios are shown in Table2 along with the average estimation error obtained as

$$\epsilon_{avg} = \frac{1}{N}\sum_{i=1}^{N} 100 \left\| \frac{\mathbf{d}_a - \mathbf{d}_{id}}{\mathbf{d}_a} \right\| \tag{22}$$

where $\mathbf{d}_a$ is the analytically computed damage and $\mathbf{d}_{id}$ is the estimated damage. The percentage error is subsequently averaged over all N numbers of performed experiments. The fifth column of Table2 lists the average estimation errors (see Equation (22) for all successful cases of damage identification. The FA index is also found to be satisfactorily low. The variation of the FA index for different noise and damage severity levels are plotted in Figure 9.

TABLE 2 False alarm index and corresponding damage estimation error for different case studies.

Case no	Damaged elements	Noise %	Damage %	ϵ_{avg} %	FA index
1	5-6	2	20	4.5571	0.01
2	5-6	5	20	14.6546	0.04
3	5-6	2	40	5.0730	0
4	5-6	5	40	15.49859	0.02
5	7-35	2	20	7.9311	0
6	7-35	5	20	15.7133	0.03
7	7-35	2	40	6.2483	0
8	7-35	5	40	14.8812	0.05
9	28-34	2	20	8.6794	0.02
10	28-34	5	20	13.3312	0.07
11	28-34	2	40	4.4365	0.02
12	28-34	5	40	9.2184	0.03
13	5-18	2	20	4.4730	0
14	5-18	5	20	12.1497	0.02
15	5-18	2	40	5.9450	0
16	5-18	5	40	8.9278	0.03
17	35-36	2	20	8.3915	0.04
18	35-36	5	20	12.1867	0.06
19	35-36	2	40	5.7502	0
20	35-36	5	40	9.1487	0.02
21	5-25,5-37	2	20	5.0473	0
22	5-25,5-37	5	20	13.3613	0.01
23	5-25,5-37	2	40	9.8339	0.01
24	5-25,5-37	5	40	6.1643	0.02
25	8-29,8-9	2	20	5.4004	0
26	8-29,8-9	5	20	9.2479	0
27	8-29,8-9	2	40	4.8179	0
28	8-29,8-9	5	40	10.2790	0.02
29	3-39,3-18	2	20	2.1617	0.01
30	3-39,3-18	5	20	9.2265	0.04
31	3-39,3-18	2	40	3.5420	0
32	3-39,3-18	5	40	8.0384	0.03

It should be noted here that the nodal stiffness is a function of all the member stiffnesses attached to that particular node. Thus, even though the member has undergone considerable damage, its contribution to the nodal stiffness deterioration is mostly small (cf. Figure 8, where 40% or 20% damage in member is only able to cause approximately 25% or 10% deterioration in nodal stiffness). Thus, this method is limited to certain levels of damage in the members that can cause significant change in the nodal stiffness.

Evidently from Figure 9, it can be observed that with small magnitude damage (<20%) or due to more noise in the measurement (>5%), the precision in damage intensity

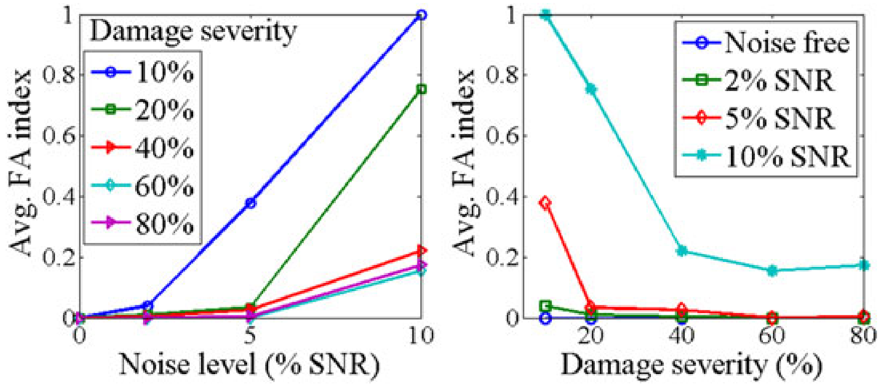

FIGURE 9 Study of false alarm for increasing noise level and damage severity

identification deteriorates, increasing the probability of false alarm. This is quite justified because small damage often fails to put a prominent signature on the measurement resulting in some undamaged elements falsely identified as slightly damaged due to noise. However, the proposed method is found not to be causing significantly high numbers of false alarm for damage levels ⩾20% and noise ⩽5%. The negligibly small false alarm probability can still be avoided either by denser instrumentation or by recursive identification of the same system.

5 | CONCLUSION

This article successfully developed a cDEKF for online damage identification in large civil infrastructure systems from noisy ambient response data. Comparative studies established the efficacy of the proposed algorithm over existing PEKF- and JEKF-based parameter identification algorithms. The possibility of unrealistic estimation due to the high dimensionality in the civil engineering systems was avoided by placing bounds on parameter in the constrained gain optimization scheme. Unlike other existing constrained filtering techniques, the proposed methodology employed constrained optimization to estimate a suboptimal Kalman gain that satisfies the feasibility condition for the estimated parameters.

Numerical examples, performed on a shear frame building and a space truss, demonstrated the proposed method's prompt and precise detection capability. Due to the formulation of the problem, the damage localization can only be achieved within sensor resolution. The chances of raising false alarm is also investigated and found to be within acceptable limits. Being a Kalman filtering-based parameter identification technique, this algorithm inherently assumes Gaussianity in the parameters and in the process that in turn restricts the algorithm to be used for the systems with non-Gaussian parameters.

REFERENCES

[1] H. Li, F. Zhang, Y. Jin. *Struct. Control Health Monit.* **2014**, *21*(7), 1100.
[2] S. Li, H. Li, Y. Liu, C. Lan, W. Zhou, J. Ou. *Struct. Control Health Monit.* **2014**, *21*(2), 156.
[3] M. Hoshiya, E. Saito. *J. Eng. Mech.* **1984**, *110*(12), 1757.
[4] O. Maruyama, M. Shinozuka, M. K. Daigaku, Program EXKAL2 for identification of structural dynamic systems, National Center for Earthquake Engineering Research **1989**.
[5] O. Maruyama, M. Hoshiya, in Structural Safety and Reliability: ICOSSAR, CA, USA, **2001**.
[6] T. Sato, K. Takei, in Proc. Structural Safety and Reliability: ICOSSAR, Kyoto, Japan, **1997**, *387*.
[7] R. E. Kalman. *J. Basic Eng.* **1960**, *82*(1), 35.
[8] S. F. Schmidt. *J. Guid. Control Dyn.* **1981**, *4*(1), 4.
[9] M. S. Grewal, A. P. Andrews, *Kalman Filtering: Theory and Practice using MATLAB*, John Wiley & Sons, New York, USA **2011**.
[10] A. Gelb, *Applied Optimal Estimation*, MIT press, Massachusetts, USA **1974**.
[11] S. J. Julier, J. K. Uhlmann. *Proc. IEEE* **2004**, *92*(3), 401.
[12] G. Welch, G. Bishop, An introduction to the kalman filter. University of North Carolina, Department of Computer Science. TR 95-041, Chapel Hill, NC, USA, **1995**.
[13] R. Ghanem, Shinozuka M. *J. Eng. Mech.* **1995**, *121*(2), 255.
[14] M. Shinozuka, R. Ghanem. *J. Eng. Mech.* **1995**, *121*(2), 265.
[15] J. N. Yang, S. Lin. *J. Eng. Mech.* **2005**, *131*(3), 290.
[16] J. N. Yang, S. Lin, H. Huang, L. Zhou. *Struct. Control Health Monit.* **2006**, *13*(4), 849.
[17] J. Yang, S. Pan, H. Huang. *Struct. Control Health Monit.* **2007**, *14*(3), 497.
[18] M. Wu, A. W. Smyth. *Struct. Control Health Monit.* **2007**, *14*(7), 971.
[19] E. N. Chatzi, A. W. Smyth. *Struct. Control Health Monit.* **2013**, *20*(7), 1081.
[20] I. Yoshida, Damage detection using monte carlo filter based on non-gaussian noise, in Structural Safety and Reliability: ICOSSAR, CA, USA, **2001**.
[21] H. Cox. *IEEE Trans. Autom. Control* **1964**, *9*(1), 5.
[22] R. E. Kopp, R. J. Orford. *AIAA J.* **1963**, *1*(10), 2300.
[23] S. S. Haykin, S. S. Haykin, S. S. Haykin, *Kalman Filtering and Neural Networks*, Wiley Online Library, New York, USA **2001**.
[24] A. Corigliano, S. Mariani. *Comput. Method. Appl. M.* **2004**, *193*(36), 3807.
[25] L. Ljung. *IEEE Trans. Autom. Control* **1979**, *24*(1), 36.
[26] L. Ljung, T. Söderström, *Theory and Practice of Recursive Identification*, MIT Press, Cambridge, Massachusetts **1983**.
[27] L. Nelson, E. Stear. *IEEE Trans. Autom. Control* **1976**, *21*(1), 94.
[28] E. A. Wan, A. T. Nelson. *Adv. Neural. Inf. Process Syst.* **1996**, *9*, 793.
[29] E. A. Wan, A. T. Nelson. *Dual extended Kalman filter methods. Kalman filtering and neural networks*, Wiley: New York **2001**, 123.
[30] C. Cheng, D. Cebon. *Vehicle Syst. Dyn.* **2011**, *49*(1-2), 399.
[31] G. Nævdal, L. M. Johnsen, S. I. Aanonsen, E. H. Vefring. *SPE J.* **2005**, *10*(01), 66–74.
[32] G. L. Plett. *J. Power Sources* **2004**, *134*(2), 277.

[33] S. Sen, B. Bhattacharya. *Struct. Infrastruct. E.* **2016**, *13*(2), 1.

[34] S. Sen, B. Bhattacharya. *Acta Mech.* **2016**, *227*(8), 2099.

[35] P. Vachhani, R. Rengaswamy, V. Gangwal, S. Narasimhan. *AIChE J.* **2005**, *51*(3), 946.

[36] S. J. Julier, J. J. LaViola. *IEEE Trans. Sig. Process.* **2007**, *55*(6), 2774.

[37] L. S. Wang, Y. T. Chiang, F. R. Chang. *IEE P. Control Theor. Ap.* **2002**, *149*(6), 525.

[38] D. M. Walker. *Int. J. Bifurc. Chaos* **2006**, *16*(04), 1067.

[39] D. Simon. *IET Control Theory Appl.* **2010**, *4*(8), 1303.

[40] S. Ungarala, E. Dolence, K. Li. Proceedings of the Eighth International IFAC Symposium on Dynamics and Control of Process Systems, IFAC, Cancun, Mexico **2007**, *2*, 63.

[41] D. Simon, T. L. Chia. *IEEE Trans. Aerosp. Electron. Syst.* **2002**, *38*(1), 128.

[42] N. Gupta, R. Hauser. *arXiv preprint arXiv:0709.2791* **2007**.

[43] J. Prakash, B. Huang, S. L. Shah. *Comput. Chem. Eng.* **2014**, *65*, 9.

[44] D. Simon, D. L. Simon. *Int. J. Syst. Sci.* **2010**, *41*(2), 159.

[45] C. B. Yun, J. H. Yi, E. Y. Bahng. *Eng. Struct.* **2001**, *23*(5), 425.

[46] J. T. Kim, N. Stubbs. *J. Struct. Eng.* **1995**, *121*(10), 1409.

How to cite this article: Sen S., and Bhattacharya B. (2016), Online structural damage identification technique using constrained dual extended Kalman filter, *Struct Control Health Monit*, doi:10.1002/stc.1961

APPENDIX

Analytical derivation of Kalman gain

Consider the linearized state space model of a dynamic system defined in discrete time domain as described by Equation 4. For a given noisy measurement $\mathbf{y}_k$, the estimation of states $\hat{\mathbf{x}}_{k|k}$ using Kalman filter is performed in two consecutive steps. In the first step ("Prediction step"), the previous estimate $\hat{\mathbf{x}}_{k-1|k-1}$ is propagated through the state transition matrix $\mathbf{A}_k$ to obtain a one step ahead prediction $\tilde{\mathbf{x}}_{k|k-1}$ of the states given information up to and including $(k-1)$th time step. This predicted estimate is subsequently corrected in the next step (i.e., "Correction step") using mismatch in predicted and actual measurement at kth time step. This is achieved by a gain matrix $\mathbf{K}_k$ (namely, "Kalman gain"), which updates the state prediction $\tilde{\mathbf{x}}_{k|k-1}$ to give corrected estimate $\hat{\mathbf{x}}_{k|k}$.

$$\begin{array}{lll} \textbf{Prediction step:} & & \tilde{\mathbf{x}}_{k|k-1} = \mathbf{A}_k\hat{\mathbf{x}}_{k-1|k-1} \\ \textbf{Correction step:} & \text{Feedback:} & \epsilon_k = \mathbf{y}_k - \mathbf{C}_k\tilde{\mathbf{x}}_{k|k-1}; \\ & \text{Update:} & \hat{\mathbf{x}}_{k|k} = \tilde{\mathbf{x}}_{k|k-1} + \mathbf{K}_k\epsilon_k \end{array} \tag{A1}$$

With Kalman filtering, in each iteration, we seek an optimal gain matrix $\mathbf{K}_k$ that minimizes the covariance of the error in the estimated states. This covariance of error between actual and estimated states can be estimated as $COV\{\mathbf{x}_k - \hat{\mathbf{x}}_{k|k}\}$ denoted as $\hat{\mathbf{P}}_{k|k}$:

$$\hat{\mathbf{P}}_{k|k} = COV\left\{\mathbf{x}_k - \left\{\tilde{\mathbf{x}}_{k|k} + \mathbf{K}_k(\mathbf{y}_k - \mathbf{C}_k\tilde{\mathbf{x}}_{k|k-1})\right\}\right\} \tag{A2}$$

Expanding $\mathbf{y}_k$ as $\mathbf{y}_k = \mathbf{C}_k\mathbf{x}_k + \mathbf{w}_k$ (see Equation 4) and rearranging the component terms in the previous equation, the following expression is obtained for state covariance estimate $\hat{\mathbf{P}}_{k|k}$ as a function of gain matrix $\mathbf{K}_k$.

$$\hat{\mathbf{P}}_{k|k} = (\mathbf{I} - \mathbf{K}_k\mathbf{C}_k)\tilde{\mathbf{P}}_{k|k-1}(\mathbf{I} - \mathbf{K}_k\mathbf{C}_k)^T - \mathbf{K}_k\mathbf{R}_k\mathbf{K}_k^T \tag{A3}$$

where $\mathbf{R}_k = COV\{\mathbf{w}_k\}$ is the measurement noise covariance matrix. $\tilde{\mathbf{P}}_{k|k-1} = COV\{\mathbf{x}_k - \tilde{\mathbf{x}}_{k|k-1}\}$ is the predicted covariance matrix obtained by propagating prior covariance estimate $\hat{\mathbf{P}}_{k-1|k-1}$ through the system model as

$$\tilde{\mathbf{P}}_{k|k-1} = \mathbf{A}_k\hat{\mathbf{P}}_{k-1|k-1}\mathbf{A}_k^T; \tag{A4}$$

In order to satisfy minimum error covariance in state estimate, the gradient of $\hat{\mathbf{P}}_{k|k}$ with respect to $\mathbf{K}_k$ is equated to zero, which gives optimal Kalman gain $\mathbf{K}_k$ as

$$\mathbf{K}_k = \frac{\mathbf{C}_k^T\tilde{\mathbf{P}}_{k|k-1}}{\mathbf{C}_k\tilde{\mathbf{P}}_{k|k-1}\mathbf{C}_k^T + \mathbf{R}_k} \tag{A5}$$

This is the analytical derivation of the Kalman gain matrix that, in each step of filtering, updates the predicted state estimate to give the current estimate of states.